

# Defining cortical frequency tuning with recurrent excitatory circuitry

Bao-hua Liu<sup>1,2,6</sup>, Guangying K Wu<sup>1,3,6</sup>, Robert Arbuckle<sup>1,5</sup>, Huizhong W Tao<sup>1,4</sup> & Li I Zhang<sup>1,2</sup>

**Neurons in the recipient layers of sensory cortices receive excitatory input from two major sources: the feedforward thalamocortical and recurrent intracortical inputs. To address their respective functional roles, we developed a new method for silencing cortex by competitively activating GABA<sub>A</sub> while blocking GABA<sub>B</sub> receptors. In the rat primary auditory cortex, *in vivo* whole-cell recording from the same neuron before and after local cortical silencing revealed that thalamic input occupied the same area of frequency-intensity tonal receptive field as the total excitatory input, but showed a flattened tuning curve. In contrast, excitatory intracortical input was sharply tuned with a tuning curve that closely matched that of suprathreshold responses. This can be attributed to a selective amplification of cortical cells' responses at preferred frequencies by intracortical inputs from similarly tuned neurons. Thus, weakly tuned thalamocortical inputs determine the subthreshold responding range, whereas intracortical inputs largely define the tuning. Such circuits may ensure a faithful conveyance of sensory information.**

Although many aspects of the representation and processing functions of neurons in the recipient layers of cortex appear to reflect converging thalamocortical inputs<sup>1–5</sup>, the functional roles and the underlying patterns of thalamocortical and, in particular, intracortical excitatory inputs remain unsolved<sup>6–9</sup>. Extensive efforts have been made to understand the thalamocortical contribution to cortical responses. These previous studies can be mostly categorized into two types: those that directly compared the response properties between simultaneously recorded neurons in the thalamus and cortex<sup>1,10–12</sup> and those that isolated thalamocortical input by preventing spiking of cortical neurons<sup>2,13–17</sup>. The first type of studies mostly used extracellular recordings and identified putatively connected thalamic and cortical units on the basis of the temporal correlation between their spikes. This approach provides information on the tuning properties of individual thalamic and cortical neurons, as well as the nature of the connection between them. A recent study in the somatosensory cortex<sup>5</sup>, which paired extracellular recording of thalamic neurons with intracellular recording of cortical cells, suggests that cortical neurons receive a number of weak, but synchronously activated, thalamic inputs, which show tuning properties similar to the recorded cortical neuron. However, as the pattern underlying divergent output connections made by a single thalamic neuron or convergent thalamic inputs made on a single cortical neuron remains largely unknown, it is difficult to determine the respective functional roles of thalamocortical and intracortical inputs.

The second type of study depends on an effective silencing of the cortex without affecting thalamocortical transmission. Three methods have been previously used to silence the cortex: (i) cortical application of muscimol, an agonist of GABA<sub>A</sub> receptors, to prevent neuronal

spiking<sup>13–15</sup>, (ii) cooling the cortex (4–14 °C) to block spike generation in neurons<sup>2,17,18</sup> and (iii) electrical stimulation of the cortex to produce a long inhibition widow (>100 ms) following excitation, during which spikes cannot be generated<sup>16</sup>. However, all of these methods are expected to have impacts on thalamocortical presynaptic transmission. Electrical stimulation can result in complex presynaptic effects such as short-term depression or facilitation. Although the mechanism underlying cooling-induced action-potential block is not yet clear, it is probable that both the action potential spread in axons and presynaptic vesicle release will also be affected by a marked temperature decrease. Microinjection, iontophoresis or perfusion of muscimol have more often been applied to silence intracortical connections<sup>13–15</sup>. It was assumed that muscimol was a highly specific agonist to GABA<sub>A</sub> receptors. However, this view has been challenged by recent findings that muscimol can activate GABA<sub>B</sub> receptors at relatively low concentrations and can reduce synaptic transmission through presynaptic GABA<sub>B</sub> receptors<sup>19</sup>.

In this work, we developed a new pharmacological method for silencing the cortex. By simultaneously blocking GABA<sub>B</sub> receptors with a specific antagonist, we were able to largely prevent the nonspecific effect of muscimol on presynaptic transmission. By applying *in vivo* whole-cell voltage-clamp recording in the rat primary auditory cortex (A1), we examined tone-evoked synaptic responses in layer 4 neurons before and after local cortical silencing. We found that thalamocortical inputs determine the area of the synaptic frequency-intensity tonal receptive field (TRF), whereas intracortical excitatory inputs largely define the frequency tuning by selectively amplifying responses at preferred frequencies of the cortical cell.

<sup>1</sup>Zilkha Neurogenetic Institute, <sup>2</sup>Department of Physiology & Biophysics, <sup>3</sup>Neuroscience Graduate Program and <sup>4</sup>Department of Ophthalmology, Keck School of Medicine, University of Southern California, 1501 San Pablo Street, Los Angeles, California 90033, USA. <sup>5</sup>Present address: Department of Child & Adolescent Psychiatry, School of Medicine, New York University, 550 First Avenue, New York, New York 10016, USA. <sup>6</sup>These authors contributed equally to this work. Correspondence should be addressed to: L.I.Z. (liizhang@usc.edu).

Received 19 September; accepted 16 October; published online 11 November 2007; doi:10.1038/nn2012

## RESULTS

## Silencing cortex with a cocktail of muscimol and SCH50911

To understand how thalamocortical and intracortical synaptic inputs contribute to the processing of individual cortical neurons, we developed a cocktail pharmacological method to effectively silence intracortical connections, while largely preserving thalamocortical synaptic transmission. Previously, cortical application of muscimol has been used to prevent spiking of cortical neurons<sup>13–15</sup>. However, recent studies suggest that muscimol can activate GABA<sub>B</sub> receptors at a relatively low concentration ( $EC_{50} = 25 \mu\text{M}$ )<sup>19</sup>. Because GABA<sub>B</sub> receptors exist on thalamocortical axons, cortical muscimol application will result in a dramatic reduction of evoked transmitter release from these axons<sup>20</sup> (Fig. 1a). Cortical microinjection of muscimol or baclofen, a specific agonist of GABA<sub>B</sub> receptors, largely eliminated tone-evoked field potentials recorded in the cortex. To overcome the nonspecific effect of muscimol on presynaptic transmission, we applied SCH50911, a specific antagonist of GABA<sub>B</sub> receptors, together with muscimol. This substantially restored the magnitude of tone-evoked field potentials (Fig. 1a). Application of SCH50911 alone slightly increased the amplitude of field-potential responses (Fig. 1a) and prolonged tone-evoked spiking activity (Supplementary Fig. 1 online), but did not change the shape of spike TRFs of cortical neurons (Supplementary Fig. 1). This is consistent with the late, prolonged inhibition that is mediated by postsynaptic GABA<sub>B</sub> receptors.

Considering the competitive binding between muscimol and SCH50911 and GABA<sub>A</sub> and GABA<sub>B</sub> receptors, respectively, we derived an optimized concentration ratio for the coapplied SCH50911 and muscimol (1.5:1) to achieve an effective activation of GABA<sub>A</sub> receptors and a blockade of GABA<sub>B</sub> receptors (see Methods and Supplementary Note 1 online for detailed calculation). After slowly injecting about 10–20 nl of the cocktail solution into the cortex, firing of cortical cells in a horizontal distance of 500  $\mu\text{m}$  was effectively blocked (spike count was reduced by >95%), as indicated by the extracellular multiunit recordings (Fig. 1b). This effect can last for at least 3 h (data not shown). Because the highest density of local intracortical excitatory input comes from neurons within a 500- $\mu\text{m}$  radius<sup>6,21,22</sup> and because the size of rat A1 is about 1–2 mm<sup>2</sup> (ref. 23), we believe that this local injection method is effective at silencing the majority of intracortical connections, although some long-distance connections may not be affected. As a control, when the cortex was injected with the vehicle solution (artificial cerebrospinal fluid, ACSF), no significant effect was observed ( $n = 5$ ,  $t$ -test,  $P > 0.5$ ) on tone-evoked cortical field potentials (data not shown).

To examine the effect of local cortical silencing on the receptive field properties of single cortical neurons, we carried out *in vivo* whole-cell voltage-clamp recordings on excitatory pyramidal neurons in layer 4 of A1

(premapped with extracellular recording, see Methods) shortly after cortical injection of muscimol or the mixture of muscimol and SCH50911. Excitatory synaptic responses evoked by pure tones of various frequencies and intensities were recorded with the neuron clamped at  $-70 \text{ mV}$ . The excitatory synaptic TRF was reconstructed after the recording. In muscimol-treated cortices, only traces of synaptic responses were observed in a small tonal-responsive area (Fig. 1c, left). On the contrary, in cocktail-treated cortices, excitatory synaptic responses with large amplitudes were observed (Fig. 1c, right). The bandwidth of an excitatory synaptic TRF measured at a 60-dB sound pressure level (SPL) was not significantly different ( $t$ -test,  $P > 0.3$ ) from that observed in normal A1 or control A1 where ACSF was injected (Fig. 1d). The local silencing of A1 under our experimental condition did not affect the response properties in the auditory thalamus that projects to A1, as multiunit spike TRFs in the ventral division of the medial geniculate body (MGBv) did not change noticeably after cortical injection of the cocktail (Fig. 1e,f). This well-restricted drug effect in the cortex may be attributed to the small volume of drug application in our experiments. The above population studies suggest that the shapes of the excitatory synaptic TRFs of neurons in the input layers of A1 are primarily determined by thalamocortical input. The apparently reduced bandwidth of excitatory

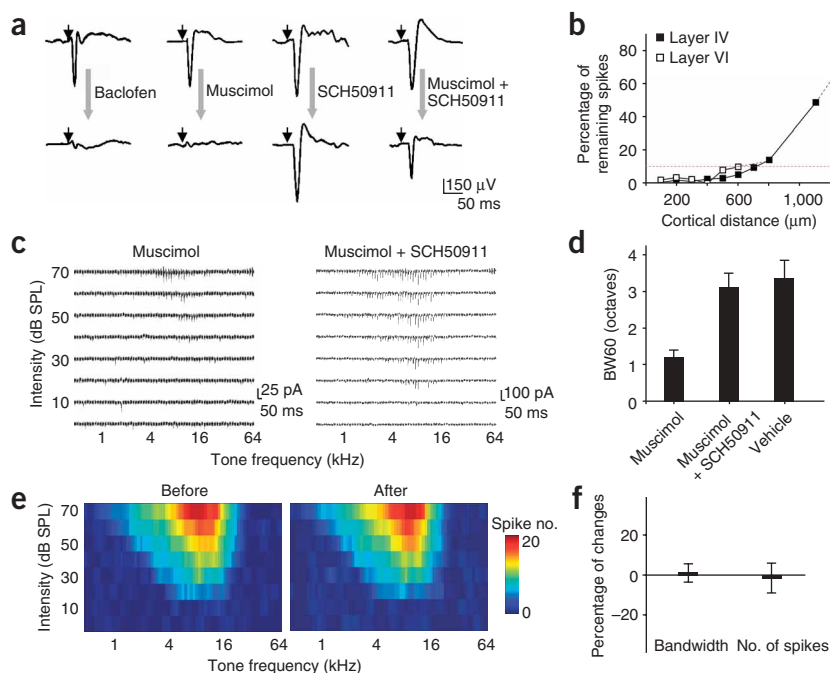


**Figure 1** Specific silencing of local intracortical connections with a cocktail pharmacological method. (a) Tone-evoked field potentials recorded in A1 before (top) and after (bottom) cortical injection of muscimol (1 mM), baclofen (1 mM), SCH50911 (1.5 mM) or a cocktail of muscimol (1 mM) and SCH50911 (1.5 mM). The small arrow marks the onset of tone stimulus. (b) Effective blocking of cortical spikes by the muscimol and SCH50911 (4:6 mM) cocktail in both layer 4 and layer 6 in a horizontal distance of 500  $\mu\text{m}$  from the injection site (see Methods). Multiunit tone-evoked spikes were detected by extracellular recordings. The red dotted line indicates a 90% reduction in spike count. (c) Example excitatory synaptic TRFs of A1 neurons obtained shortly after muscimol (left) and cocktail (right) injection. Each small trace represents the response (recorded at  $-70 \text{ mV}$ ) to a tone of a particular frequency and intensity. (d) Average bandwidth of synaptic TRF measured at 60 dB (BW60) in A1 injected with muscimol ( $n = 9$ ), cocktail ( $n = 8$ ) or vehicle (ACSF,  $n = 7$ ). Error bars represent s.d. (e) Spike TRF (average of four repetitions) for a recording site in the MGBv before and after cortical injection of the cocktail. Color represents the number of spikes evoked by a tone stimulus. (f) Percentage change in the bandwidth and spike count for tone-evoked spikes (measured at 60 dB) in the MGBv before and after cortical cocktail application ( $n = 6$  sites). Error bars represent s.d.

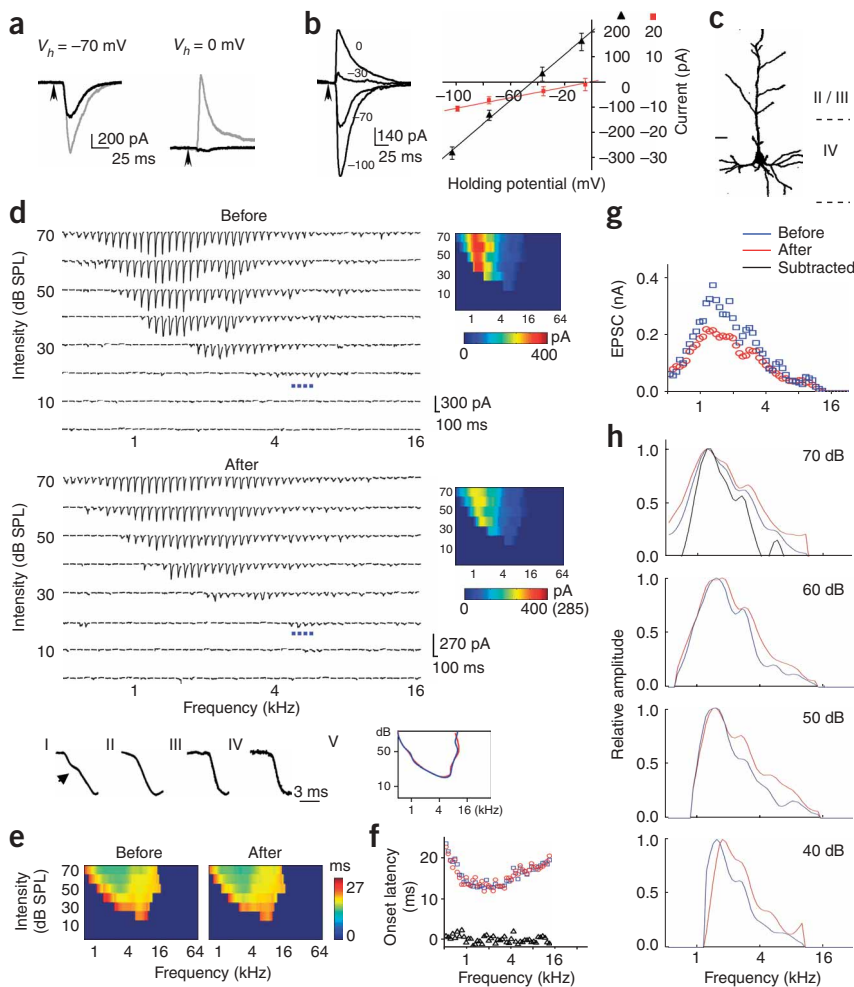


**Figure 2** Changes in excitatory synaptic TRF after local cortical silencing. **(a)** Excitatory (left) and inhibitory (right) synaptic currents evoked by a tone of 1.5 kHz and 70 dB before (gray) and after (black) cocktail application. **(b)** Left, synaptic currents (average of five repeats) evoked by a tone of 1.9 kHz and 70 dB, recorded at different holding potentials. Right,  $I$ - $V$  curves ( $V$  is corrected) for synaptic currents averaged in a 20–22.5-ms window after the stimulus onset (black) and a 0–1-ms window after the response onset (red). **(c)** Morphology of the recorded cell. Scale bar, 20  $\mu$ m. **(d)** TRF of excitatory synaptic currents before (average of two repeats) and after (four repeats) silencing. Blue dots mark the responses at the intensity threshold (20 dB). The color maps show the average amplitudes. Number in the bracket indicates the original scale before correction. Bottom, the rising phase of average synaptic response to a 1.3-kHz tone at 60 dB before (I) and after (II) cortical silencing or to a 5.6-kHz tone at 20 dB before (III) and after (IV) cortical silencing. **(e)** Color map of onset latencies of evoked excitatory currents. **(f)** Onset latencies (at 70 dB) before (blue) and after (red) cocktail application. Triangle represents the difference. **(g)** Amplitudes of responses before (blue) and after (red) cocktail application at 70 dB. **(h)** Tuning curves of excitatory currents at four different tone intensities. The black line represents the tuning curve of subtracted responses.

synaptic TRFs in the presence of muscimol (**Fig. 1d**, ref. 14) may be largely attributed to the nonspecific effect of muscimol on presynaptic GABA<sub>B</sub> receptors.

### Thalamocortical input determines the area of synaptic TRFs

To further examine the pattern of thalamocortical and intracortical excitatory inputs and their roles in determining frequency tuning, we recorded synaptic TRFs from the same A1 neuron before and after cortical silencing (for example, **Fig. 2**). The cell was clamped at  $-70$  mV and then at  $0$  mV to record tone-evoked excitatory and inhibitory currents, respectively (**Fig. 2a**). The linearity of the  $I$ - $V$  curve suggests that the cell was reasonably clamped (**Fig. 2b**, see **Supplementary Note 2** online for detailed discussion). The injection of the muscimol and SCH50911 cocktail was made at a cortical site about 500  $\mu$ m below the pial surface and had a horizontal distance from the recorded cell of 100  $\mu$ m. Tone-evoked inhibitory currents were eliminated after the injection (**Fig. 2a**), consistent with silencing of intracortical inhibitory connections. The amplitude of excitatory currents was substantially reduced (**Fig. 2a**), which can be attributed to silencing of intracortical excitatory connections and nonspecific effects of cocktail application, including those caused by changes in series resistance and input resistance (**Supplementary Table 1** online, see **Supplementary Note 2** for detailed calculation).

We assumed that tone-evoked excitatory responses at the subthreshold intensity threshold (20 dB in this particular cell) mostly originated

from monosynaptic thalamocortical synapses. This assumption is supported by three observations. First, the reduction in the amplitude of excitatory currents was the smallest at the subthreshold intensity threshold. Second, the multiunit spike TRFs recorded from the same site before silencing had a higher intensity threshold (30 dB, **Supplementary Fig. 2** online), suggesting that the synaptic currents at the subthreshold intensity threshold are unlikely to have originated from local intracortical inputs. Third, the kinetics of the rising phase of response currents at the intensity threshold remained mono-phased after cocktail application, whereas those of response currents to best-frequency tones above the intensity threshold changed from bi-phased to mono-phased, consistent with synaptic inputs of two sources that have different onsets (**Fig. 2d**, bottom). Thus, on the basis of the relative change in the amplitude of average response at the intensity threshold after the cocktail application ( $-29\%$ ), we estimated that the cocktail application had caused a 29% nonspecific reduction of the response amplitude in this cell (see **Supplementary Note 2** for more discussion). The amplitude of each excitatory response after cortical silencing was then corrected by a factor of 1.41 (see Methods).

From the excitatory TRF after the correction (shown by the bottom color map in **Fig. 2d**), it is apparent that after cortical silencing there is no noticeable change in the range of responding frequencies at various testing intensities, or in the intensity threshold (**Fig. 2d**). This result further supports the notion that thalamocortical input primarily defines the shapes of excitatory synaptic TRFs. In addition, the graded amplitude of thalamocortical responses indicates that the cortical neuron is innervated by a number of thalamic neurons, with each possessing spike TRFs in the frequency-intensity range defined by the excitatory synaptic TRF of this cell.

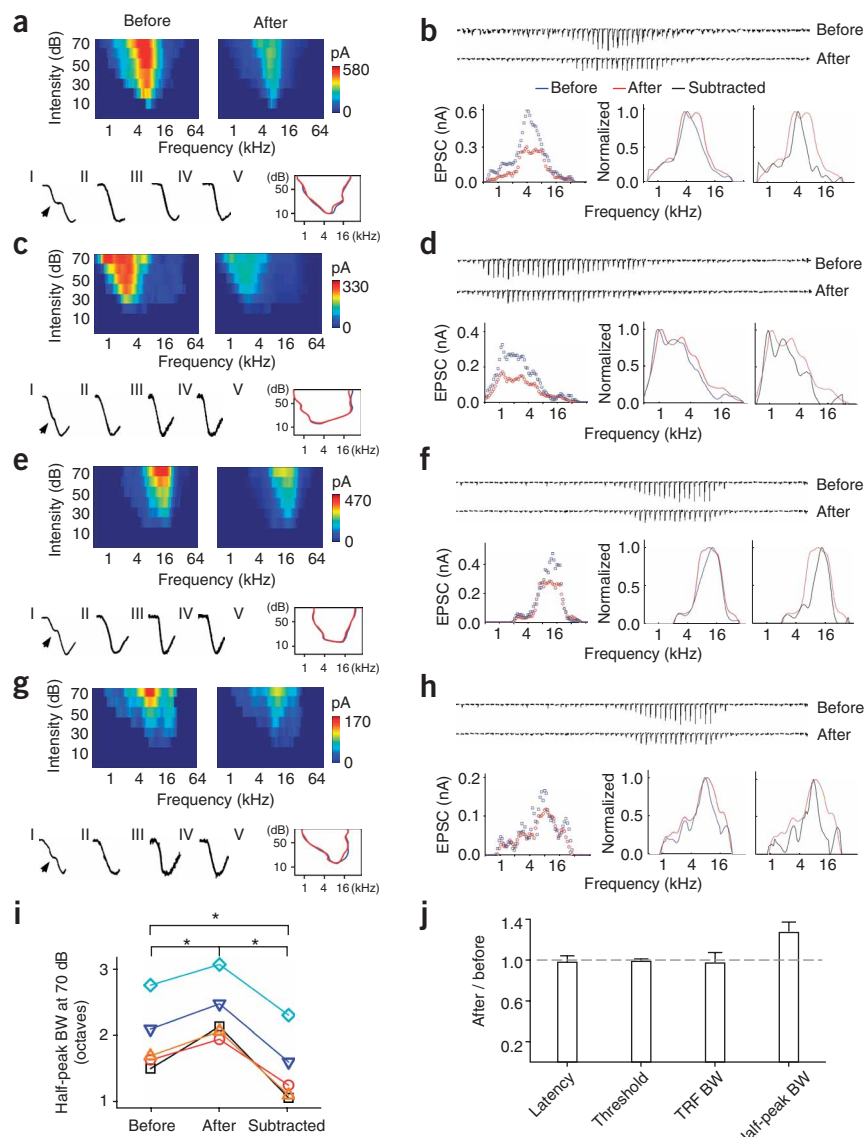


**Figure 3** Intracortical inputs are more sharply tuned than thalamocortical inputs. (**a–h**) Changes in excitatory synaptic TRFs in another four cells. (**a,c,e,g**) Top, color maps represent the excitatory synaptic TRFs before and after cocktail application. Bottom, kinetics of the rising phase of synaptic currents (I–IV). The curved line outlines the boundary of the synaptic TRF before (blue) and after (red) cocktail application (V). (**b,d,f,h**) Top, excitatory synaptic currents evoked by tones (at 70 dB) of different frequencies before and after cocktail application. The amplitudes of currents after application are corrected. Bottom, excitatory tuning curves at 70 dB before (blue) and after (red) cortical silencing. Data are presented as in **Figure 2** (**a–h**). Black lines are for the subtracted inputs. (**i**) Half-peak bandwidths of tuning curves at 70 dB for total excitatory (before), thalamic (after) and intracortical inputs (subtracted). Data points from the same cell are connected with lines ( $n = 5$ , paired  $t$ -test,  $* P < 0.01$ ). (**j**) Average ratio of onset latency, intensity threshold of excitatory synaptic TRF, bandwidth at 10 dB above the intensity threshold (TRF BW) and half-peak bandwidth of tuning curve at 70 dB (half-peak BW) between after and before values. Error bars represent s.d.

tuning. Intracortical connections provide both excitatory and inhibitory inputs. Previous data have suggested that intracortical inhibitory input can sharpen spike tuning curves through an analogous ‘iceberg’ effect<sup>25–27</sup> and that it may also increase the temporal precision of spike responses by temporally following excitatory input with a brief delay<sup>26</sup>. In contrast, the functional role of intracortical excitatory input remains largely unknown. Here, we compared the frequency tuning curves before and after cortical silencing, which are depicted by the envelope of amplitudes of responses at certain intensity. It appears that the shape of the tuning curves became more flattened after cortical silencing, as reflected by an increase in the half-peak

We next examined the onset latency for each response in the TRF before and after cortical silencing (**Fig. 2e**). A clear pattern of onset-latency values was observed in the TRF, with the shortest latencies appearing at high intensities and clustering around preferred frequencies, and the longest latencies appearing at the periphery of the TRF. This is reminiscent of a similar finding in visual cortical receptive fields<sup>24</sup>, from which it was proposed that long-latency responses are a result of intracortical spread of visual activity. In the present study, however, there was no significant change ( $n = 47$ , paired  $t$ -test,  $P > 0.9$ ) in either short or long onset latencies after cortical silencing (**Fig. 2f**), suggesting that the onset latency is determined mostly by thalamocortical input. The variation in onset latency is likely attributable to variation in the conduction velocity subcortically and in the integration time for action potential generation in subcortical neurons.

#### Weakly tuned thalamic and sharply tuned intracortical inputs

The analysis above indicates that thalamocortical input primarily determines the area of the synaptic TRF. We next examined the role of thalamic and intracortical inputs in determining cortical frequency

bandwidth of the tuning curves (**Fig. 2g,h**). The flat or plateau peak of the thalamocortical tuning curve (**Fig. 2g**) indicates that thalamocortical inputs are, in fact, weakly tuned.

A total of five cortical neurons were examined in this manner (another four cells are shown in **Fig. 3**). In all of these neurons, there was no noticeable change in the range of responding frequencies or in the intensity threshold after cortical silencing (**Fig. 3a,c,e,g,j** and **Supplementary Fig. 3** online). At the mean time, the frequency tuning curve became flattened, showing both a broad plateau peak that covered the preferred frequencies of the cell and a broader half-peak bandwidth than that of the total inputs (**Fig. 3b,d,f,h–j**). We further quantified the pattern of intracortical excitatory inputs by subtracting the thalamocortical component from the total excitatory responses (**Figs. 2h** and **3b,d,f,h**, black lines). The tuning curves for excitatory intracortical inputs showed the same preferred frequencies as those for total excitatory inputs, but their half-peak bandwidths were significantly narrower than those for both the total and thalamocortical inputs ( $n = 5$ , paired  $t$ -test,  $P < 0.01$ , **Fig. 3i**). These results demonstrate that local intracortical excitatory input is more sharply

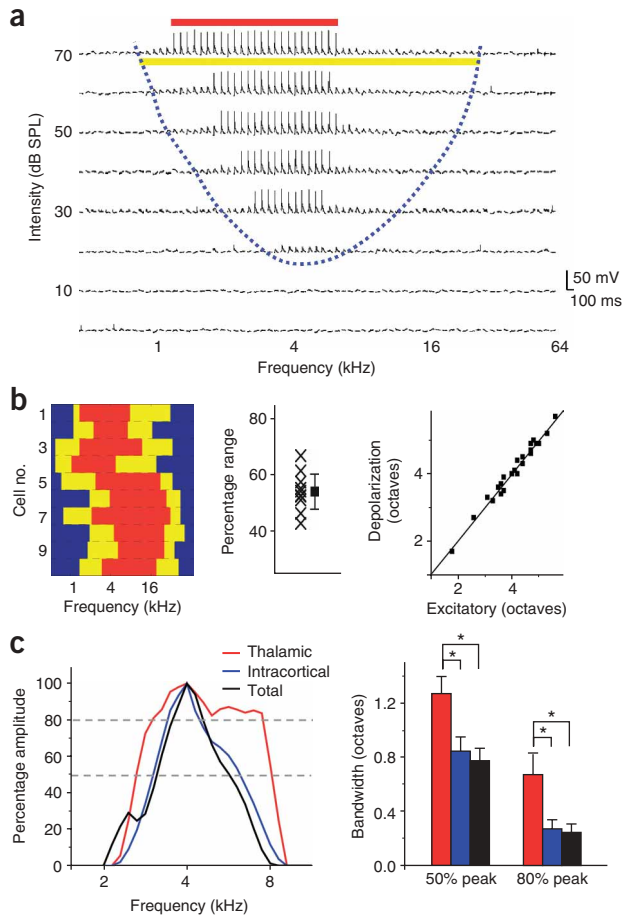


**Figure 4** Similarly tuned intracortical inputs sharpen the frequency tuning curve in layer 4. **(a)** Membrane potential responses to tones of various frequencies and intensities, recorded under current clamp from a representative A1 neuron. Blue dashed line delineates the boundary for the TRF of tone-evoked membrane depolarizations. The yellow and red lines indicate the frequency range (at 70 dB) for subthreshold and spike responses, respectively. **(b)** Left, frequency range for subthreshold (yellow) and spike (red) responses at 70 dB of ten cells detected with current-clamp recording. Middle, percentage frequency range for spike responses in the range for membrane potential responses. Each cross represents one cell. The square represents the average of all cells ( $\pm$ s.d.). Right, for 24 cells in which both voltage-clamp and current-clamp recordings were obtained, the frequency range (at 70 dB) of membrane depolarizations (ordinate) closely matched that of excitatory synaptic currents (abscissa). **(c)** Left, normalized tuning curves after thresholding in the estimated suprathreshold response range for total excitatory (black), thalamocortical (red) and intracortical (blue) input in a cell. Right, average bandwidths at 50% and 80% peak amplitude of 'suprathreshold' tuning curves ( $n = 5$  cells, paired  $t$ -test,  $* P < 0.03$ ). Error bars represent s.d.

tuned than thalamocortical input and has a greater contribution at the preferred frequencies of the cell.

### Recurrent excitation largely defines frequency tuning

What is the role of intracortical input in determining the frequency tuning of cortical cells? The preferred frequencies of intracortical excitatory input closely matched the plateau peak of the thalamocortical tuning curve (Figs. 2g and 3b,d,f,h), suggesting that the intracortical inputs arose from a group of similarly tuned neurons. We carried out further whole-cell current-clamp recordings to compare subthreshold and spike TRFs in the same cortical neuron. We found that the frequency range for spike responses was narrower than that for excitatory synaptic input (Fig. 4a,b). The average frequency range for spike responses measured at 60 dB was about  $54 \pm 7\%$  (mean  $\pm$  s.d.,  $n = 10$ ) of that for excitatory synaptic input, consistent with previous findings that spike threshold sharpens neuronal tuning for many stimulus attributes<sup>27–31</sup>. As a result, each intracortical excitatory input, which depends on a cortical cell's firing, will inevitably have a narrower frequency range than direct thalamocortical input. When excitatory intracortical inputs with similar tuning properties are pooled, they can selectively amplify excitatory responses at their preferred frequencies.

We next compared the contribution of thalamocortical and intracortical inputs to the synaptic tuning curve over the frequency range of suprathreshold responses, which reflects the spiking probability of the cell under fluctuating membrane potentials. The suprathreshold response range was estimated by the derived membrane-potential responses (determined by synaptic responses before cortical silencing,

see Methods) that showed an increase of  $> 20$  mV. The tuning curves of the total, the thalamocortical and the derived intracortical inputs were then thresholded in the defined suprathreshold frequency range and normalized. The bandwidths of these thresholded tuning curves were compared. In the suprathreshold frequency range, the tuning curve of intracortical input closely matched that of total excitatory input (Fig. 4c). In contrast, the thalamocortical tuning curve was significantly broader ( $n = 5$ , paired  $t$ -test,  $P < 0.03$ ). This finding further supports the notion that, although thalamocortical input determines the subthreshold responding range, the frequency tuning of the cortical neuron is largely defined by more narrowly tuned intracortical excitatory input.

### DISCUSSION

Extensive efforts have been made to address the role of feedforward thalamocortical input in determining the response properties or the representation and processing functions of layer 4 neurons in the sensory cortex<sup>1–5</sup>. Experimental studies in the primary visual, somatosensory and auditory cortices all suggest that the response properties of layer 4 cortical neurons can be explained by the convergence of thalamic inputs<sup>1–5,9,32</sup>. However, both the extent to which response properties of cortical neurons represent those of thalamic inputs and the functional pattern of these inputs have not been fully addressed. Moreover, the contribution of recurrent intracortical excitatory connections to cortical processing remains largely unclear. Modeling studies suggest that they may function as a cortical amplifier for the feedforward excitation<sup>6</sup>, and may account for the emergence of contrast-invariant orientation selectivity in the visual cortex<sup>7</sup>. In contrast, a recent study in the somatosensory cortex suggests that cortical amplification may not be required, as layer 4 neurons receive a large number of synchronous sensory-driven thalamic inputs, which together can be strong enough to trigger spike responses<sup>5</sup>.

In the present study, by using a cortical silencing method that leaves thalamocortical transmission largely unaffected, we were able to isolate the thalamocortical component underlying the synaptic TRFs of cortical neurons. We conclude that thalamocortical input determines the range of subthreshold responses, as synaptic TRFs cover the same area before and after cortical silencing, although the amplitude of each excitatory response is reduced. This reduction can be attributed to the silencing of intracortical excitatory connections and nonspecific effects caused by the cocktail application (see **Supplementary Note 2** for detailed discussion). By taking into account the nonspecific reduction and correcting the response amplitudes accordingly, we estimate that for the largest tone-evoked excitatory response

(saturating response) in the TRF, about  $61 \pm 11\%$  (mean  $\pm$  s.d.) of the response has a thalamocortical origin and  $39 \pm 11\%$  has a cortical origin ( $n = 5$  cells). These values are comparable to the estimation in the cat primary visual cortex that thalamic input comprises about 46% of the total excitatory input<sup>16</sup>. The smallest tone-evoked responses after cortical silencing presumably originate from single thalamic inputs, and they can generate membrane depolarizations of about 0.5–1 mV. We can thus estimate that each saturating response evoked by a pure tone stimulus consists of  $18 \pm 6$  synchronous thalamic inputs (averaged from the five cells), consistent with the findings in the somatosensory cortex that many synchronous thalamic inputs are underlying sensory-evoked responses of single cortical neurons<sup>5</sup>. Although we could not infer the total number of thalamic projections made onto an A1 neuron, the excitatory TRF after cortical silencing has revealed a functional pattern of thalamic inputs.

The comparison between the tuning curves of total excitatory, thalamocortical and derived intracortical input showed that weakly tuned thalamocortical input has been remarkably sharpened by intracortical input. The peak of the thalamocortical tuning curve is broad and flat, suggesting a low level of selectivity if responses at the peak are suprathreshold. The tuning curve of intracortical input is sharper, and the tuning curve of total excitatory input in the spiking frequency range more closely resembles that of intracortical input than that of thalamocortical input. If we consider the synaptic tuning curve to be a distribution of spiking probability, we can conclude that intracortical input defines the shape of the spike tuning curve, in a manner similar to adding a pyramid on top of a flat base (Supplementary Fig. 4 online). In other words, intracortical input reconstitutes the sharpness of frequency tuning in the cortex. The similar preferences of thalamocortical and intracortical tunings imply a recurrent circuitry in which local similarly tuned neurons excite each other (Supplementary Fig. 4). These intracortical inputs selectively amplify the thalamocortical signal and determine the optimal stimulus of the cortical cell. In conclusion, our results are consistent with models in which intracortical recurrent excitation determines stimulus selectivity of cortical neurons. We propose that by combining the breadth of feedforward excitation and selectivity of recurrent excitation, a reliable and faithful conveyance of subcortically processed sensory information to the cortex can be ensured.

## METHODS

**Animal preparation and extracellular recording.** All experimental procedures used in this study were approved by the Animal Care and Use Committee of the University of Southern California. Experiments were carried out in a sound-proof booth (Acoustic Systems) as described previously<sup>23,27,33</sup>. Female Sprague-Dawley rats  $\sim 3$  months old and weighing 250–300 g were anaesthetized with ketamine and xylazine (see discussion in Supplementary Note 2). Pure tones (0.5–64 kHz at 0.1-octave intervals, 25-ms duration, 3-ms ramp) at eight 10-dB-spaced sound intensities were delivered to the contralateral ear. Multiunit spike responses were recorded with parylene-coated tungsten micro-electrodes (2 M $\Omega$ , FHC) placed 500–600  $\mu$ m below the pial surface. The number of tone-evoked spikes was counted in a window of 10–30 ms from the onset of tone stimulus. Auditory cortical mapping was carried out by sequentially recording from an array of cortical sites. The location of A1 was identified as previously described<sup>23,27,33</sup>. For recording in the auditory thalamus, we systematically mapped the MGB with extracellular recordings in a three-dimensional manner by varying the depth and  $xy$  coordinates of the electrode. We identified the MGBv, which projects to A1 (ref. 34), according to its tonotopy of frequency representation and the relatively sharper spike TRFs seen there than in other MGB divisions<sup>35</sup>.

**Local cortical silencing.** Muscimol can activate both GABA<sub>A</sub> ( $EC_{50} = 1.7 \mu$ M) and GABA<sub>B</sub> ( $EC_{50} = 25 \mu$ M) receptors<sup>19</sup>. For effective silencing of the cortex

with minimum impact on presynaptic transmission, we derived an optimized concentration ratio for muscimol and SCH50911 on the basis of their competitive binding to GABA<sub>A</sub> or GABA<sub>B</sub> receptors:

$$A + Gb \xrightarrow{Kb_1} A \cdot Gb \quad [A \cdot Gb] = [A] \times [Gb] \times [Kb_1] \quad (1)$$

$$B + Gb \xrightarrow{Kb_2} B \cdot Gb \quad [B \cdot Gb] = [B] \times [Gb] \times [Kb_2] \quad (2)$$

$$A + Ga \xrightarrow{Ka_1} A \cdot Ga \quad [A \cdot Ga] = [A] \times [Ga] \times [Ka_1] \quad (3)$$

$$B + Ga \xrightarrow{Ka_2} B \cdot Ga \quad [B \cdot Ga] = [B] \times [Ga] \times [Ka_2] \quad (4)$$

where  $A$  is for SCH90511,  $B$  for muscimol,  $Gb$  for GABA<sub>B</sub> receptor and  $Ga$  for GABA<sub>A</sub> receptor.  $[A]$ ,  $[B]$ ,  $[Ga]$  and  $[Gb]$  represent the concentration of  $A$ ,  $B$ ,  $Ga$  and  $Gb$ , respectively.

Here,  $EC_{50}$  or  $IC_{50}$  values are used to calculate binding constants to reflect the functional effects of binding on channel opening or blocking:  $Kb_1 = 1/(1 \mu$ M),  $Kb_2 = 1/(25 \mu$ M),  $Ka_1 \leq 1/(900 \mu$ M) and  $Ka_2 = 1/(1.7 \mu$ M). We consider  $\leq 5\%$  receptors bound to be no significant effect, and  $\geq 95\%$  bound as being fully effective. Under these conditions, a ratio of 1.5:1 (SCH50911: muscimol) was chosen (see Supplementary Note 1 for detailed calculation). A high concentration (6:4 mM) was used to effectively silence a relatively large cortical region. Pharmacological reagents (dissolved in ACSF containing Fast Green) or control solution (ACSF containing Fast Green) were injected through a glass micropipette with a tip opening of  $\sim 2$ – $3 \mu$ m in diameter, attached via polyethylene tubing to a syringe. The pressure inside the tubing was monitored with a pressure gauge. After premapping A1, the pipette was inserted to a depth of 500–600  $\mu$ m beneath the cortical surface near the center of A1 and was controlled by a motorized micromanipulator. Solutions were injected under a pressure of 3–4 psi for 5 min. The injected volume was estimated to be around 10–20 nl, as measured with mineral oil. Without applying pressure, there was no apparent leakage of intrapipette solution, as there was no leakage of green color and no change in cortical responses. The staining by Fast Green was monitored under the surgical microscope, and spread fast under the injection pressure, covering a cortical area with a radius of 500–600  $\mu$ m by the end of the injection. This meant that the initial concentration of injected cocktail was quickly diluted by about 50-fold, as estimated from the change in volume. Experiments were normally completed within 30 min of drug injection, with one drug experiment being carried out in each animal preparation. Cortical responses largely recovered 7 h after the injection, probably as a result of the slow diffusion of drugs in the cortex<sup>13</sup>.

**In vivo whole-cell recording.** Whole-cell recordings<sup>25–27,33,36,37</sup> were obtained from neurons located 500–700  $\mu$ m beneath the cortical surface, corresponding to the input layers of the auditory cortex<sup>38</sup>. For voltage-clamp recordings, the patch pipette (4–7 M $\Omega$ ) contained 125 mM cesium-gluconate, 5 mM TEA-chloride, 4 mM magnesium ATP, 0.3 mM GTP, 10 mM phosphocreatine, 10 mM HEPES, 1 mM EGTA, 2 mM CsCl, 2 mM QX-314, pH 7.2, and 0.5% biocytin. The whole-cell and pipette capacitance were completely compensated for, and the initial series resistance (20–50 M $\Omega$ ) was 50–60% compensated for, to achieve an effective series resistance of 10–25 M $\Omega$ . Signals were filtered at 5 kHz and sampled at 10 kHz. For current-clamp recordings to examine spikes, the same patch pipette was used, containing 125 mM potassium gluconate, 4 mM magnesium ATP, 0.3 mM GTP, 10 mM phosphocreatine, 10 mM HEPES, 1 mM EGTA, pH 7.2, and 0.5% biocytin. Histological staining of the recorded cells<sup>39–41</sup> after recording indicated that the whole-cell recording method under our current condition was biased for sampling pyramidal neurons. In this study, the measured membrane potentials of the recorded neurons ranged from  $-61$  to  $-72$  mV, with a mean of  $-63.8$  mV.

To obtain tone-evoked excitatory inputs, the cells were clamped directly at  $-70$  mV, which is around the reversal potential of inhibitory currents ( $E_i$ ), as described in our previous studies<sup>25,27,33</sup>. Cortical cells can be reasonably clamped before and after cocktail application with a clamping deviation of  $\pm 5$  mV (see Supplementary Figs. 5–7 and Supplementary Note 2 online). For a few cases when both excitatory and inhibitory TRFs were obtained before cortical silencing, we derived the excitatory synaptic conductance,  $Ge(t)^{25–27,29,33,41,42}$ , by  $I(t, V) = Gr(V - Er) + Ge(t)(V - Ee) + Gi(t)(V - Ei)$ ,

where  $V$  is the clamping voltage,  $G_r$  is the resting conductance,  $E_r$  is the resting potential,  $E_e$  and  $E_i$  are the reversal potentials for excitatory and inhibitory synaptic currents, respectively, and  $I(t, V)$  is the current amplitude under  $V$ .  $V(t)$  is given by  $V(t) = V_c - R_s \times I(t)$ , where  $R_s$  is the effective series resistance and  $V_c$  is the clamping voltage applied. The liquid junction potential is estimated to be 12 mV. We found that varying  $E_i$  values between  $-65$  and  $-75$  mV did not change the conclusion of this study.

**Data analysis.** Tone-evoked excitatory synaptic or membrane potential responses were identified according to their onset latencies and peak amplitudes. Only responses with an onset and peak occurring within 7–30 ms from the onset of tone stimulus and with a peak amplitude at least threefold greater than the s.d. of baseline fluctuation were considered to be tone-evoked responses. The response onset latency was taken as the time point in the rising phase of the response curve, where the amplitude change was two folds of the s.d. of baseline fluctuation<sup>25</sup>. The boundaries of synaptic TRFs were defined according to the consistency of tone-evoked responses in 2–4 repetitions and the continuity of responses with the change of frequency and intensity. For color maps of synaptic TRFs, repetitions were averaged and only the pixels in the determined TRF boundary were labeled<sup>27,33</sup>.

The estimated membrane potential responses ( $V_{est}$ ) for the voltage-clamp recordings before the drug application were derived using  $V_{est}(t) = [GrV_r + Ge(t)E_e + Gi(t)E_i]/[Gr(t) + Ge(t) + Gi(t)]$ , where  $V_r$  is the resting membrane potential. Because  $G_i$  was not determined for most of the cells in this study, we derived the membrane potential changes that were caused by excitatory inputs alone, and estimated the spike threshold to be 20 mV above the resting membrane potential.

To correct for the nonspecific effects of the cocktail application, we averaged tone-evoked responses at the intensity threshold of synaptic TRFs before and after cortical silencing. We assumed that these responses mostly originated from monosynaptic thalamic inputs. The relative reduction in their amplitudes ( $r$ ) can be largely explained by the changes in input and series resistances after cocktail application (Supplementary Table 1, see Supplementary Note 2 for detailed calculation) and thus is used as a reflection of nonspecific effects of cocktail application. The amplitude of each response was then normalized by a correction factor of  $1/(1 - r)$ . It is worth noting that varying the correction factor by  $\pm 25\%$  does not qualitatively change the conclusion of this study.

Note: Supplementary information is available on the Nature Neuroscience website.

#### ACKNOWLEDGMENTS

This work was supported by grants to L.I.Z. from the US National Institutes of Health/National Institute on Deafness and Other Communication Disorders, the Searle Scholar Program, the Esther A. & Joseph Klingenstein Fund, Inc., and the David and Lucile Packard Foundation.

#### AUTHOR CONTRIBUTIONS

L.I.Z. conceived the study. G.K.W. and B.L. carried out the *in vivo* experiments and data analysis. B.L. modeled the effects of cocktail application on synaptic responses. R.A. was involved in current-clamp recordings. L.I.Z. and H.W.T. supervised the project and wrote the paper.

Published online at <http://www.nature.com/natureneuroscience>

Reprints and permissions information is available online at <http://npg.nature.com/reprintsandpermissions>

1. Reid, R.C. & Alonso, J.M. Specificity of monosynaptic connections from thalamus to visual cortex. *Nature* **378**, 281–284 (1995).
2. Ferster, D., Chung, S. & Wheat, H. Orientation selectivity of thalamic input to simple cells of cat visual cortex. *Nature* **380**, 249–252 (1996).
3. Chung, S. & Ferster, D. Strength and orientation tuning of the thalamic input to simple cells revealed by electrically evoked cortical suppression. *Neuron* **20**, 1177–1189 (1998).
4. Miller, L.M., Escabi, M.A., Read, H.L. & Schreiner, C.E. Functional convergence of response properties in the auditory thalamocortical system. *Neuron* **32**, 151–160 (2001).
5. Bruno, R.M. & Sakmann, B. Cortex is driven by weak but synchronously active thalamocortical synapses. *Science* **312**, 1622–1627 (2006).
6. Douglas, R.J., Koch, C., Mahowald, M., Martin, K.A. & Suarez, H.H. Recurrent excitation in neocortical circuits. *Science* **269**, 981–985 (1995).
7. Somers, D.C., Nelson, S.B. & Sur, M. An emergent model of orientation selectivity in cat visual cortical simple cells. *J. Neurosci.* **15**, 5448–5465 (1995).

8. Miller, K.D., Pinto, D.J. & Simons, D.J. Processing in layer 4 of the neocortical circuit: new insights from visual and somatosensory cortex. *Curr. Opin. Neurobiol.* **11**, 488–497 (2001).
9. Alonso, J.M. & Swadlow, H.A. Thalamocortical specificity and the synthesis of sensory cortical receptive fields. *J. Neurophysiol.* **94**, 26–32 (2005).
10. Miller, L.M., Escabi, M.A., Read, H.L. & Schreiner, C.E. Spectrotemporal receptive fields in the lemniscal auditory thalamus and cortex. *J. Neurophysiol.* **87**, 516–527 (2002).
11. Miller, L.M., Escabi, M.A. & Schreiner, C.E. Feature selectivity and interneuronal cooperation in the thalamocortical system. *J. Neurosci.* **21**, 8136–8144 (2001).
12. Martinez, L.M. *et al.* Receptive field structure varies with layer in the primary visual cortex. *Nat. Neurosci.* **8**, 372–379 (2005).
13. Fox, K., Wright, N., Wallace, H. & Glazewski, S. The origin of cortical surround receptive fields studied in the barrel cortex. *J. Neurosci.* **23**, 8380–8391 (2003).
14. Kaur, S., Lazar, R. & Metherate, R. Intracortical pathways determine breadth of subthreshold frequency receptive fields in primary auditory cortex. *J. Neurophysiol.* **91**, 2551–2567 (2004).
15. Zhang, Y. & Suga, N. Corticofugal amplification of subcortical responses to single tone stimuli in the mustached bat. *J. Neurophysiol.* **78**, 3489–3492 (1997).
16. Chung, S. & Ferster, D. Strength and orientation tuning of the thalamic input to simple cells revealed by electrically evoked cortical suppression. *Neuron* **20**, 1177–1189 (1998).
17. Volgushev, M., Vidyasagar, T.R., Chistiakova, M., Yousef, T. & Eysel, U.T. Membrane properties and spike generation in rat visual cortical cells during reversible cooling. *J. Physiol. (Lond.)* **522**, 59–76 (2000).
18. Villa, A.E. *et al.* Corticofugal modulation of the information processing in the auditory thalamus of the cat. *Exp. Brain Res.* **86**, 506–517 (1991).
19. Yamauchi, T., Hori, T. & Takahashi, T. Presynaptic inhibition by muscimol through GABAB receptors. *Eur. J. Neurosci.* **12**, 3433–3436 (2000).
20. Porter, J.T. & Nieves, D. Presynaptic GABA<sub>A</sub> receptors modulate thalamic excitation of inhibitory and excitatory neurons in the mouse barrel cortex. *J. Neurophysiol.* **92**, 2762–2770 (2004).
21. Roerig, B. & Chen, B. Relationships of local inhibitory and excitatory circuits to orientation-preference maps in ferret visual cortex. *Cereb. Cortex* **12**, 187–198 (2002).
22. Marino, J. *et al.* Invariant computations in local cortical networks with balanced excitation and inhibition. *Nat. Neurosci.* **8**, 194–201 (2005).
23. Zhang, L.I., Bao, S. & Merzenich, M.M. Persistent and specific influences of early acoustic environments on primary auditory cortex. *Nat. Neurosci.* **4**, 1123–1130 (2001).
24. Bringuiet, V., Chavane, F., Glaeser, L. & Fregnac, Y. Horizontal propagation of visual activity in the synaptic integration field of area 17 neurons. *Science* **283**, 695–699 (1999).
25. Zhang, L.I., Tan, A.Y., Schreiner, C.E. & Merzenich, M.M. Topography and synaptic shaping of direction selectivity in primary auditory cortex. *Nature* **424**, 201–205 (2003).
26. Wehr, M. & Zador, A.M. Balanced inhibition underlies tuning and sharpens spike timing in auditory cortex. *Nature* **426**, 442–446 (2003).
27. Tan, A.Y., Zhang, L.I., Merzenich, M.M. & Schreiner, C.E. Tone-evoked excitatory and inhibitory synaptic conductances of primary auditory cortex neurons. *J. Neurophysiol.* **92**, 630–643 (2004).
28. Carandini, M. & Ferster, D. Membrane potential and firing rate in cat primary visual cortex. *J. Neurosci.* **20**, 470–484 (2000).
29. Anderson, J.S., Carandini, M. & Ferster, D. Orientation tuning of input conductance, excitation and inhibition in cat primary visual cortex. *J. Neurophysiol.* **84**, 909–926 (2000).
30. Priebe, N. & Ferster, D. Direction selectivity of excitation and inhibition in simple cells of the cat primary visual cortex. *Neuron* **45**, 133–145 (2005).
31. Wilent, W.B. & Contreras, D. Stimulus-dependent changes in spike threshold enhance feature selectivity in rat barrel cortex neurons. *J. Neurosci.* **25**, 2983–2991 (2005).
32. Swadlow, H.A. & Gusev, A.G. Receptive-field construction in cortical inhibitory interneurons. *Nat. Neurosci.* **5**, 403–404 (2002).
33. Wu, G.K., Li, P., Tao, H.W. & Zhang, L.I. Nonmonotonic synaptic excitation and imbalanced inhibition underlying cortical intensity tuning. *Neuron* **52**, 705–715 (2006).
34. Winer, J.A., Miller, L.M., Lee, C.C. & Schreiner, C.E. Auditory thalamocortical transformation: structure and function. *Trends Neurosci.* **28**, 255–263 (2005).
35. Calford, M.B. & Webster, W.R. Auditory representation within principal division of cat medial geniculate body: an electrophysiology study. *J. Neurophysiol.* **45**, 1013–1028 (1981).
36. Moore, C.I. & Nelson, S.B. Spatio-temporal subthreshold receptive fields in the vibrissa representation of rat primary somatosensory cortex. *J. Neurophysiol.* **80**, 2882–2892 (1998).
37. Margrie, T.W., Brecht, M. & Sakmann, B. *In vivo*, low-resistance, whole-cell recordings from neurons in the anaesthetized and awake mammalian brain. *Pflugers Arch.* **444**, 491–498 (2002).
38. Games, K.D. & Winer, J.A. Layer V in rat auditory cortex: projections to the inferior colliculus and contralateral cortex. *Hear. Res.* **34**, 1–25 (1988).
39. Horikawa, K. & Armstrong, W.E. A versatile means of intracellular labelling: injection of biocytin and its detection with avidin conjugates. *J. Neurosci. Methods* **25**, 1–11 (1988).
40. Zhu, Y., Stornetta, R.L. & Zhu, J.J. Chandelier cells control excessive cortical excitation: characteristics of whisker-evoked synaptic responses of layer 2/3 nonpyramidal and pyramidal neurons. *J. Neurosci.* **24**, 5101–5108 (2004).
41. Hirsch, J.A., Alonso, J.M., Reid, R.C. & Martinez, L.M. Synaptic integration in striate cortical simple cells. *J. Neurosci.* **18**, 9517–9528 (1998).
42. Borg-Graham, L.J., Monier, C. & Fregnac, Y. Visual input evokes transient and strong shunting inhibition in visual cortical neurons. *Nature* **393**, 369–373 (1998).